Photoinduced Intramolecular Electron Transfer in 1,2,4,5-Tetrakis(diphenylphosphino)benzene-Bridged Os^{II}−M^{II} Dimetallic Complexes (M = Ni, Pd, Pt)

Pei-Wei Wang and Marye Anne Fox*

Department of Chemistry and Biochemistry, University of Texas, Austin, Texas 78712

Received May 13, 1994⊗

Emission quantum yields observed for the dimetallic complexes [(bpy)$_2$Os^{II}−(tppb)−M^{II}(dppb)] (M = Ni, Pd, Pt) and [(bpy)$_2$Os^{II}−(bpy)$_2$] (bpy = 2,2′-bipyridine; dppb = 1,2-bis(diphenylphosphino)benzene; tppb = 1,2,4,5-tetrakis(diphenylphosphino)benzene) reflect substantial intramolecular interaction between the component metal centers in the excited states of these complexes. The slightly shifted redox potentials and absorption spectra of the dimetallic complexes, in comparison with their monometallic models, [Os^{II}(bpy)$_2$(dppb)] and [M^{II}(dppb)$_2$] (M = Ni, Pd, Pt), are consistent with modest interactions in the ground states of these complexes, as has been observed for the analogous Ni^{II} dimetallic complexes. The quantum yields (ϕ = 0.002) and excited state lifetimes (τ = 9−12 ns) of the dimetallic complexes [(bpy)$_2$Os^{II}−(tppb)−M^{II}(dppb)] (M = Ni, Pd) were lower and shorter than those of [Os^{II}(bpy)$_2$(dppb)] (ϕ = 0.049, τ = 270 ns), as is consistent with quenching of the Os^{II} MLCT state by the second metal center. The apparent intramolecular electron transfer rate constants ($k_{et} = 3 \times 10^5 - 1 \times 10^8$ s^{-1}) for the excited states of the dimetallic complexes [(bpy)$_2$Os^{II}−(tppb)−M^{II}(dppb)] (M = Ni, Pd, Pt) correlate with calculated driving forces for electron transfer from *Os^{II} to M^{II} (M = Ni, Pd, Pt).

Introduction

Extensive studies on the excited state properties of polynuclear metal complexes have provided a better understanding of their participation in electron and energy transfer.[1] The electronic coupling between metal centers has been found to depend on the nature of the bridging ligands, e.g., for cyanide,[1c] 4,4′-bipyridine (bpy),[2a,b] 2,2′-bipyramidine,[2c,d] or 2,3-bis(2-pyridyl)pyrazine,[2e] but despite their utility as complexing ligands, phosphino ligands have rarely been characterized as bridging ligands in photoactive polynuclear metal complexes. The photophysical properties of polynuclear complexes can be tuned by different combinations of metal ions and ligands, a capability that has allowed these polynuclear complexes to be used in supramolecular arrays.[3]

Polypyridyl complexes of d^6 transition metals, e.g., Ru^{II}, Os^{II}, and Re^{I}, have long-lived, luminescent, photochemically inert ^{3}MLCT excited states.[4] The excited states of these complexes are known to undergo both reductive and oxidative quenching.[4] Meyer and co-workers also demonstrated that replacing one of the polypyridyl ligands (σ-donating ligand) with various phosphine ligands (π-acceptor) in the polypyridyl−Os^{II} complexes enhanced the excited state lifetimes and quantum yields of the ^{3}MLCT excited states.[5] Although the phosphine ligand does not itself absorb light, it does cause an increase of the energy of the ^{3}MLCT state of the complex and, consequently, slows the complex's rate of nonradiative decay.

In this paper, the syntheses and characterization of various 1,2,4,5-tetrakis(diphenylphosphino)benzene-bridged dimetallic complexes **1** (bpy = 2,2′-bipyridine; dppb = 1,2-bis(diphenylphosphino)benzene) are reported. These complexes were prepared by metalation of the bis(bipyridyl)osmium(II) complex **2**. Interaction between metal centers in **1** (in the ground and excited states) is characterized here by cyclic voltammetry, absorption spectroscopy, emission spectroscopy, and laser flash photolysis. Previous work in our group has shown that intramolecular thermal coupling of metal centers by 1,2,4,5-tetrakis(diphenylphosphino)benzene is weak in a series of analogous dimetallic Ni^{II} complexes,[6] but the ability of this

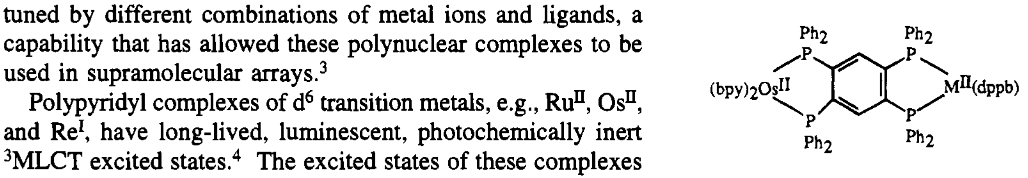

1a, M = Ni

1b, M = Pd

1c, M = Pt

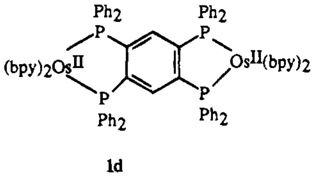

1d

⊗ Abstract published in *Advance ACS Abstracts*, December 1, 1994.

(1) (a) Wasielewski, M. R. In *Photoinduced Electron Transfer*; Fox, M. A., Chanon, M., Eds.; Elsevier: New York, 1988; Part A, p 161. (b) Scandola, F.; Indelli, M. T. *J. Phys. Chem.* **1993**, *97*, 3328. (c) Scandola, F.; Argazzi, R.; Bignozzi, C. A.; Chiorboli, C.; Indelli, M. T.; Rampi, M. A. *Coord. Chem. Rev.* **1993**, *125*, 283. (d) Kalyanasundaram, K.; Nazeeruddin, K. Md. *Inorg. Chem.* **1990**, *29*, 1888. (e) Murphy, W. R., Jr.; Brewer, K. J.; Gettliffe, G.; Peterson, J. D. *Inorg. Chem.* **1989**, *28*, 81. (f) Schmehl, R. H.; Auerbach, R. A.; Wacholtz, W. F. *J. Phys. Chem.* **1988**, *92*, 6202. (g) Schanze, K. S.; Neyhart, G. A.; Meyer, T. J. *J. Phys. Chem.* **1986**, *90*, 2182. (h) Cooley, L. F.; Haedford, C. E. L.; Elliott, C. M.; Kelley, D. F. *J. Am. Chem. Soc.* **1988**, *110*, 6673.

(2) (a) Goldsby, K. A.; Meyer, T. J. *Inorg. Chem.* **1984**, *23*, 3003. (b) Curtis, J. C.; Bernstein, J. S.; Meyer, T. J. *Inorg. Chem.* **1985**, *24*, 385. (c) Rillema, D. P.; Mack, K. B. *Inorg. Chem.* **1982**, *21*, 3849. (d) Hunziker, M.; Ludi, A. J. *J. Am. Chem. Soc.* **1977**, *99*, 7370. (e) Brauenstein, C. H.; Baker, A. D.; Streakas, T. C.; Gafney, H. D. *Inorg. Chem.* **1984**, *23*, 857.

(3) (a) Balzani, V.; Scandola, F. *Supramolecular Photochemistry*; Horwood: Chichester, U.K., 1991; Chapter 12. (b) Amadelli, R.; Argazzi, R.; Bignozzi, C. A.; Scandola, F. *J. Am. Chem. Soc.* **1990**, *112*, 7099. (c) Fujihira, M.; Sakomura, M.; Kamei, T. *Thin Solid Films* **1989**, *1*, 43.

(4) Kalyanasundaram, K. *Photochemistry of Polypyridine and Porphyrin Complexes*; Academic Press: London, 1992.

(5) (a) Johnson, S. R.; Westmoreland, T. D.; Casper, J. V.; Barqawi, K. R.; Meyer, T. J. *Inorg. Chem.* **1988**, *27*, 3195. (b) Kober, E. M.; Casper, J. V.; Sullivan, B. P.; Meyer, T. J. *Inorg. Chem.* **1988**, *27*, 4587. (c) Kober, E. M.; Sullivan, B. P.; Dressick, W. J.; Casper, J. V.; Meyer, T. J. *J. Am. Chem. Soc.* **1980**, *102*, 7383.

(6) Wang, P. W.; Fox, M. A. *Inorg. Chem.* **1994**, *33*, 2938.

0020-1669/95/1334-0036$09.00/0

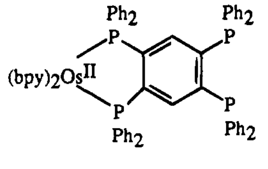

2

ligand to mix with excited states for enhanced electronic coupling has not yet been described. Because emission from the monometallic complex **3** in solution at room temperature is

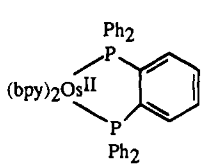

3

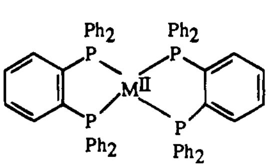

4 **(M = Ni, Pd, or Pt)**

quenched by complexes **4** (M = Ni), we have studied the photophysical properties of the corresponding dimetallic complexes **1a–c**. (The low solubility of **4** (M = Pd, Pt) in organic solvents has restricted the possibility of performing a bimolecular quenching study between **3** and **4** (M = Pd, Pt).) Because the magnitude of the thermal intermetallic coupling in the analogous dimetallic Ni^{II} complexes is modest, we can consider the excited state of **1a–c** as rigid, structurally-fixed models for an in-plane collision complex between an excited osmium complex and a monometallic quencher.

To that end, the excited state lifetimes and quantum yields for the dimetallic complexes **1a–c** are compared with those of the analogous monometallic complexes $(bpy)_2Os(dppb)$, **3**, and $[M(dppb)]_2$, **4** (M = Ni, Pd, Pt). The observed magnitude of the calculated apparent intramolecular electron transfer rate constants (k_{et}) in the excited states of the dimetallic complexes **1a–c** are discussed in relation to the relative driving force ($\Delta G°$) for electron transfer from the excited Os^{II} center to the M^{II} center (M = Ni, Pd, Pt).

Experimental Section

Physical Measurements. Electrochemical measurements were carried out with a Princeton Applied Research Model 173 potentiostat equipped with a Model 179 digital coulometer and a Model 175 universal programmer or a BAS 100 electrochemical analyzer. Typical experiments were run at 100 mV/s in CH_3CN with 0.1 M $[n\text{-}Bu_4N]PF_6$ (Sachem Inc., used as supplied) as the supporting electrolyte. For cyclic voltammetry, a Ag/AgCl wire was used as a pseudoreference electrode, a Pt wire as the counter electrode, and a Pt disk as the working electrode. Ferrocene was used as an internal standard to calibrate the observed potential (vs SCE).[7]

Proton-decoupled ^{31}P-NMR spectra were measured on a Nicolet NT-360 spectrometer, referenced to a solution of 85% H_3PO_4 in D_2O. Absorption spectra were measured on a Hewlett-Packard 8451A diode array spectrophotometer. Emission spectra were measured on a SLM Aminco SPF-500C spectrofluorometer. Emission quantum yields were determined on dry, freeze-pump-thawed (five times) or N_2-purged solutions of 0.1 M $[n\text{-}Bu]_4PF_6$ in CH_3CN relative to $[Ru(bpy)_3][PF_6]_2$ ($\phi_{em} = 0.062$)[8] at room temperature. Luminescence lifetimes were obtained by exciting the sample ($\sim 10^{-4}$ M) with a Nd-YAG laser (532 nm) as a pulsed source. The emission decay was monitored at right angles by a PTI monochromator with a R928 photomultiplier detector. The PMT output was fed into a Tektronix TDS 540 transient digitizer. Excited state lifetimes were determined by a least-squares fit of the exponential decay. Steady state photolysis was conduced in a sealed NMR tube containing a freeze-pump thawed (five times) solution of 0.1 M $[n\text{-}Bu_4N]PF_6/CD_3CN$ exposed to an unfocused 1000 W Xe lamp. Elemental analyses were obtained from Galbraith Laboratories.

Materials. 1,2-Bis(diphenylphosphino)benzene (dppb),[8] 1,2,4,5-tetrakis(diphenylphosphino)benzene (tppb),[8] $(dppb)NiCl_2$,[9] $(dppb)PdCl_2$,[10] $(dppb)PtCl_2$,[11] $(bpy)_2OsCl_2$,[5b] $(bpy)Os(dppb)(PF_6)_2$ (**3**),[5a] and $[M(dppb)_2][BF_4]_2$ (**4**, M = Ni, Pd, Pt)[6] were prepared by literature methods. $(NH_4)_2OsCl_6$, NH_4PF_6, and HBF_4 (85% solution in ether) (Aldrich) were used as received.

Bis(2,2′-bipyridine)(1,2,4,5-tetrakis(diphenylphosphino)benzene)-osmium Hexafluorophosphate, $[Os(bpy)_2(tppb)](PF_6)_2$ (2). A mixture of $(bpy)_2OsCl_2$[5b] (600 mg, 1.05 mmol) and tppb[8] (8 g, 9.83 mmol) was heated under reflux in 75 mL of 1,2-dichlorobenzene/DMF/ethylene glycol (4/1/1) for 1.5 h. To the cooled reaction mixture was added 1 g of NH_4PF_6 dissolved in 50 mL of H_2O. The organic layer was collected, and 200 mL of ether was added to precipitate the crude product. The product was purified by chromatography on basic alumina using acetonitrile/toluene (1/1) as the eluent. The first orange band was collected, and the solvent was removed under reduced pressure. The product was collected and recrystallized from 30 mL of acetone/ethanol (1/5) with 1 g of NH_4PF_6 added. The final product was vacuum-dried at 110 °C for 4 h. Yield: 900 mg (52%). ^{31}P-NMR (CD_3CN): δ 28.8 (s, Os^{II}-coordinated phosphines), −11.4 (s, noncoordinated phosphines). Anal. Calcd for $C_{74}H_{58}N_4P_6F_{12}Os{\cdot}2H_2O$: C, 54.09; H, 3.80; N, 3.41. Found: C, 53.52; H, 3.62; N, 3.18.[12a]

1,1-Bis(2,2′-bipyridine)(μ-1,2,4,5-tetrakis(diphenylphosphino)-benzene)-2-(1,2-bis(diphenylphosphino)benzene)osmiummetal Hexafluorophosphate, **$[(bpy)_2Os-(tppb)-M(dppb)][PF_6]_4$ (1a–c).** Tetrafluoroboric acid (3 equiv of an 85% solution in ether) was added to a solution of $[Os(bpy)_2(tppb)][PF_6]_2$, **2** (1 equiv), and $(dppb)MCl_2$ (M = Ni,[9] Pd,[10] Pt[10]) (1 equiv) in 60 mL of CH_2Cl_2. The resulting mixture was stirred 1 h at room temperature before the solvent was removed under reduced pressure. The solid was collected by filtration and recrystallized from 30 mL of acetone/ethanol (1/5) with 1 g of NH_4PF_6 added. The final product was vacuum-dried at 120 °C for 4 h.

1a, M = Ni. Yield: 51%. ^{31}P-NMR (CD_3CN): δ 57.8 (m, Ni^{II}-coordinated phosphines), 29.7 (s, Os^{II}-coordinated phosphines). Anal. Calcd for $C_{104}H_{82}N_4P_{10}F_{24}OsNi{\cdot}2H_2O$: C, 51.23; H, 3.39; N, 2.30. Found: C, 50.94; H, 3.46; N, 2.21.[12a]

1b, M = Pd. Yield: 73%. ^{31}P-NMR (CD_3CN): δ 53.8 (s, Pd^{II}-coordinated phosphines), 29.6 (s, Os^{II}-coordinated phosphines). Anal. Calcd for $C_{104}H_{82}N_4P_{10}F_{24}OsPd{\cdot}2H_2O$: C, 50.24; H, 3.49; N, 2.25. Found: C, 50.26; H, 3.56; N, 2.05.[12a]

1c, M = Pt. Yield: 66%. ^{31}P-NMR (CD_3CN): δ 45.3 (m, Pt^{II}-coordinated phosphines), 29.7 (s, Os^{II}-coordinated phosphines). Anal. Calcd for $C_{104}H_{82}N_4P_{10}F_{24}OsPt{\cdot}2H_2O$: C, 48.51; H, 3.37; N, 2.18. Found: C, 49.16; H, 3.53; N, 2.05.[12a]

1,1-Bis(2,2′-bipyridine)(μ-1,2,4,5-tetrakis(diphenylphosphino)-benzene)-2,2-bis(2,2′-bipyridine)diosmium Hexafluorophosphate, $[(bpy)_2Os-(tppb)-Os(bpy)_2][PF_6]_4$ (1d). A mixture of $(bpy)_2OsCl_2$[5b] (250 mg, 0.44 mmol) and tppb[8] (1 g, 1.23 mmol) was heated under reflux in 15 mL of ethylene glycol for 1.5 h. To the cooled reaction mixture was added 1 g of NH_4PF_6 dissolved in 50 mL of H_2O. The product was collected and recrystallized from 30 mL of acetone/ethanol (1/5) with 1 g of NH_4PF_6 added. The final product was vacuum-dried at 110 °C for 4 h. Yield: 350 mg (67%). ^{31}P-NMR (CD_3CN): δ 29.7 (s), 29.1 (s).[12b] Anal. Calcd for $C_{94}H_{74}N_8P_8F_{24}Os_2{\cdot}2H_2O$: C, 46.35; H, 3.06; N, 4.60. Found: C, 46.36; H, 3.22; N, 4.39.[12a]

---

(7) Bard, A. J.; Faulkner, L. R. *Electrochemical Methods: Fundamental and Applications*; Wiley: New York, 1980; p 701.

(8) Casper, J. V.; Meyer, T. J. *J. Am. Chem. Soc.* **1983**, *105*, 5583.

(9) Christina, H.; McFarlane, E.; McFarlane, W. *Polyhedron* **1988**, 1875.

(10) Levason, W.; McAuliffe, C. A. *Inorg. Chim. Acta* **1974**, *11*, 33.

(11) Levason, W.; McAuliffe, C. A. *Inorg. Chim. Acta* **1976**, *16*, 167.

(12) (a) The relative large elemental analysis errors for complexes **1a–d** and **2** (0.01–0.65 for carbon) are caused by the large molecular weights of these complexes (MW > 2000), strong chelation effects between the metal ions and phosphine ligands, their high tendencies to coordinate additional water (as shown by ^1H-NMR spectroscopy), and the relative oxidative instability of the phosphino ligands over the period required for elemental analysis. (b) The two-peak ^{31}P-NMR spectrum (with the integration ratio of 1:1) of the diosmium complex is assigned as a mixture of two diastereomers $\Delta\Lambda$ (or $\Lambda\Delta$) and $\Delta\Delta$ (or $\Lambda\Lambda$).

Table 1. Cyclic Voltammetric Peak Potentials of Complexes **1**, **3**, and **4**[a]

	potential (V vs SCE)			
complex	$Os^{II/III}$ $(\Delta E_p)^b$	$M^{II/I}$ or 0 $(\Delta E_p)^b$	$Ni^{I/0}$ $(\Delta E_p)^b$	$bpy^{0/-}$ $(\Delta E_p)^b$
1a	1.36 (70 mV)	−0.18 (50 mV) $Ni^{II/I}$	−0.45 (50 mV)	−1.30 (50 mV)
1b	1.37 (70 mV)	−0.60 (50 mV) $Pd^{II/0}$		−1.31 (60 mV)
1c	1.37 (80 mV)	−0.76 (50 mV) $Pt^{II/0}$		−1.30 (60 mV)
1d	1.43 (150 mV)			−1.27 (50 mV)
3	1.30 (70 mV)			−1.31 (60 mV)
4 (M = Ni)[c]		−0.26 (60 mV) $Ni^{II/I}$	−0.60 (60 mV) $Ni^{I/0}$	
4 (M = Pd)[c]		−0.68 (40 mV) $Pd^{II/0}$		
4 (M = Pt)[c]		−0.78 (40 mV) $Pt^{II/0}$		
$(bpy)_3Os(PF_6)_2$[d]	0.81 (60 mV)			−1.29 (60 mV)

[a] Conditions: scan rate, 100 mV/s; reference electrode, Ag/AgCl; counter electrode, Pt wire; working electrode, Pt disk; 0.1 M $[n\text{-}Bu_4N]PF_6$ in CH_3CN under N_2 at room temperature. [b] ΔE_p is the peak-to-peak separation between the cathodic and anodic waves. [c] From ref 6. [d] From ref 5a.

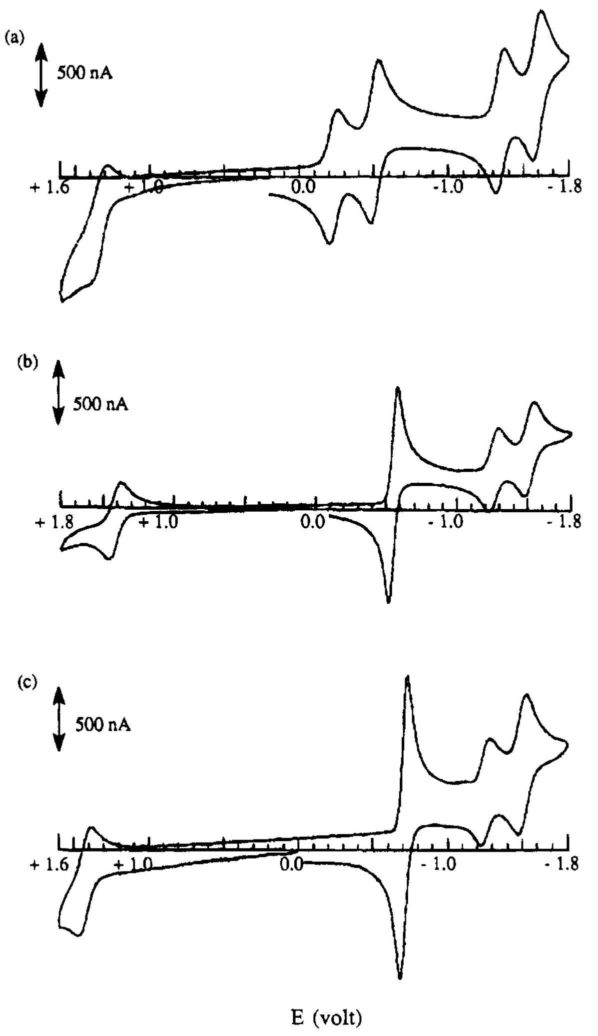

Figure 1. Cyclic voltammograms of dimetallic complexes **1**: (a) **1a** (0.1 mM); (b) **1b** (0.1 mM); (c) **1c** (0.1 mM). Conditions: scan rate, 100 mV/s; reference electrode, Ag/AgCl; counter electrode, Pt wire; working electrode, Pt disk; 0.1 M $[n\text{-}Bu_4N]PF_6$ in CH_3CN under N_2 at room temperature.

Results and Discussion

Ground State Properties. Electrochemistry. Redox chemistry of **1a**, as in eq 1, can be seen in its cyclic voltammogram, Figure 1a. In addition to the $Os^{II/III}$, $(bpy)^{0/-}$, and $(bpy)_2^{-/2-}$ couples, **1a** shows two reversible one-electron reduction waves

$$\begin{aligned}&(bpy)_2Os^{III}tppbNi^{II}(dppb) \xrightleftharpoons{e^-} (bpy)_2Os^{II}tppbNi^{II}(dppb)\\ &\xrightleftharpoons{e^-} (bpy)_2Os^{II}tppbNi^{I}(dppb) \xrightleftharpoons{e^-} (bpy)_2Os^{II}\text{-}ppbNi^{0}(dppb)\\ &\xrightleftharpoons{e^-} (bpy)(bpy)^{\ominus}Os^{II}tppbNi^{0}(dppb) \xrightleftharpoons{e^-} (bpy^{\ominus})_2Os^{II}tppbNi^{0}(dppb)_2\end{aligned} \qquad (1)$$

(Os^{II}–$Ni^{II/I}$, Os^{II}–$Ni^{I/0}$). The presence of the Os^{II} center causes a shift of the reduction peaks to somewhat less negative potentials than observed for **4** (M = Ni), presumably because the cationic Os^{II} center in the dimetallic complex **1a** exerts a net electron-withdrawing effect on the Ni^{II} couple. Similar effects have been observed for a 1,2,4,5-tetraphosphinobenzene-bridged dimetallic Ni^{II} complex in comparison with the corresponding monometallic Ni^{II} complex.[6]

Table 1 summarizes the redox potentials of various monometallic and dimetallic complexes **1a**–**d**, **3**, **4**, and $[Os^{II}(bpy)_3]$. The oxidations for the $Os^{II/III}$ couples in the phosphine-substituted Os^{II} complexes **1a**–**d** and **3** occur at potentials ~500 mV positive of the corresponding oxidation in $[Os^{II}(bpy)_3]$. The shift is as would be predicted by the change from bpy to the more π-accepting phosphine[5a] and by variation in electrostatic effects within the series. The $bpy^{0/-}$ couple is observed at nearly the same potential (~−1.30 V) for each of the complexes.

The dimetallic complexes **1b** and **1c** show slightly different electrochemical behaviors, parts b and c, respectively, of Figure 1. Both the dimetallic complexes **1b** and **1c** show a two-electron reversible reduction of Os^{II}–$M^{II/0}$ (M = Pd, Pt), eq 2. The

$$\begin{aligned}&(bpy)_2Os^{III}tppbM^{II}(dppb) \xrightleftharpoons{e^-} (bpy)_2Os^{II}tppbM^{II}(dppb)\\ &\xrightleftharpoons{2e^-} (bpy)_2Os^{II}tppbM^{0}(dppb) \xrightleftharpoons{e^-} (bpy)(bpy)^{\ominus}Os^{II}tppbM^{0}(dppb)\\ &\xrightleftharpoons{e^-} (bpy^{\ominus})_2Os^{II}tppbM^{0}(dppb)_2\\ &\qquad (M = Pd \text{ or } Pt)\end{aligned} \qquad (2)$$

reduction peaks for the Os^{II}–$Pd^{II/0}$ and Os^{II}–$Pt^{II/0}$ conversions are shifted about 80 and 20 mV, respectively, from those observed for **4** (M = Pd, Pt), Table 1. The dimetallic complex **1d** exhibits a quasi-reversible (ΔE_p = 150 mV) oxidation wave at 1.43 V, Table 1. The peak-to-peak separation indicates that **1d** undergoes two reversible one-electron oxidations ($Os^{II/III}$ and $Os^{II/III}$).[13] The first $bpy^{0/-}$ wave of **1d** occurs at a slightly less negative potential (−1.27 V) than that of **3** (−1.31 V), Table 1.

---

[13] Richardson, D. E.; Taube, H. *Inorg. Chem.* **1981**, *20*, 1278.

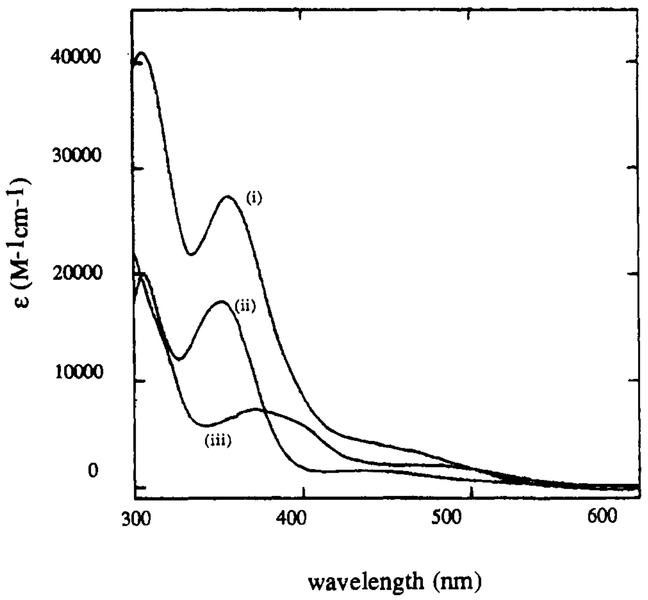

Figure 2. Absorption spectra of **1a**, **3**, and **4** (M = Ni) in 0.1 M [*n*-Bu$_4$N]PF$_6$/CH$_3$CN: (i) **1a** (2.3 × 10^{-5} M); (ii) **4** (M = Ni) (1.7 × 10^{-5} M); (iii) **3** (1.7 × 10^{-5} M).

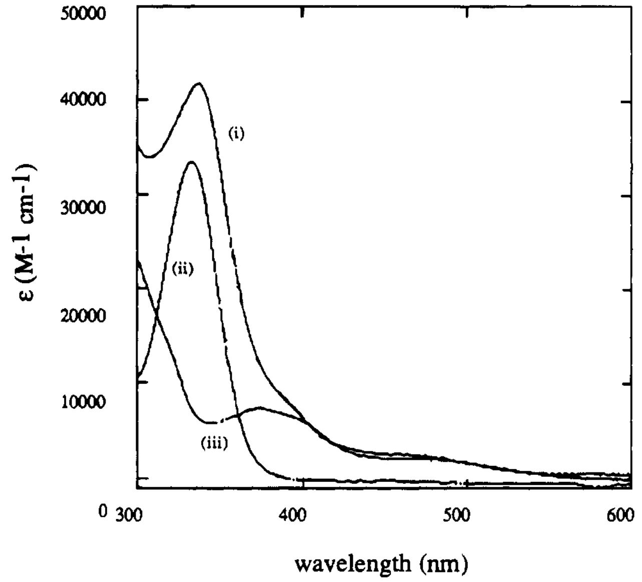

Figure 3. Absorption spectra of **1b**, **3**, and **4** (M = Pd) in 0.1 M [*n*-Bu$_4$N]PF$_6$/CH$_3$CN: (i) **1b** (2.4 × 10^{-5} M); (ii) **4** (M = Pd) (1.4 × 10^{-5} M); (iii) **3** (1.7 × 10^{-5} M).

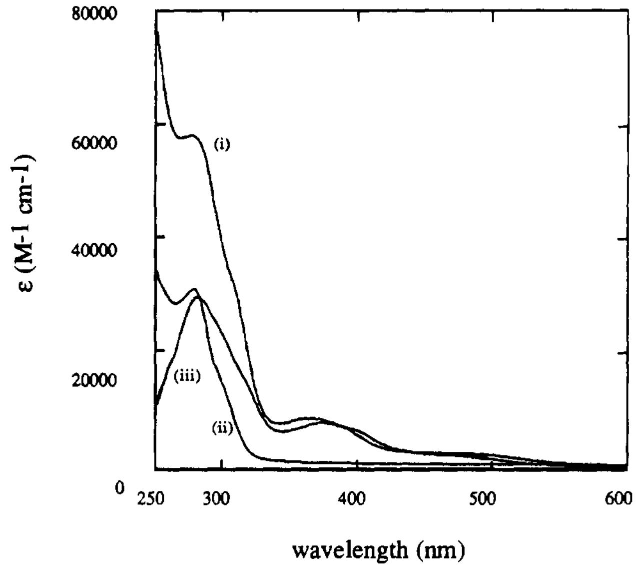

Figure 4. Absorption spectra of **1c**, **3**, and **4** (M = Pt) in 0.1 M [*n*-Bu$_4$N]PF$_6$/CH$_3$CN: (i) **1c** (1.9 × 10^{-5} M); (ii) **4** (M = Pt) (1.8 × 10^{-5} M); (iii) **3** (1.7 × 10^{-5} M).

The redox potentials of the subcomponents in the dimetallic complexes **1a–d** differ by less than 150 mV from those observed for the related monometallic complexes **3** and **4**, suggesting that only modest electronic interaction between the two metal centers in the ground state, as had been demonstrated earlier, and more rigorously, for the corresponding Ni^{II}/Pd^{II} and Ni^{II}/Pt^{II} complexes.[6] The magnitude of the intermetallic electronic coupling in **1a–d** is presumably affected by the lack of a low-lying empty orbital in the tppb-bridging ligand. No reduction of the tppb$^{0/-}$ couple for the dimetallic complexes **1a–d** is observed. Thus, the bridging phosphine ligand tppb is ineffective in providing strong coupling of the two metal centers.[13b–d]

Absorption Spectra. The absorption spectra of the dimetallic complexes **1a–c** can be quantitatively deconvoluted to components identical with the spectra of the related monometallic complexes **3** and **4** (Figures 2–4). The monometallic complex **3** exhibits MLCT (Os → bpy) bands at 470 nm (predominantly triplet in character) and about 370 nm (predominately singlet in character).[5b] The charge transfer band (Os → dppb) occurs at higher energy than does that of MLCT (Os → bpy) because of the relatively high energy of the d,π orbital in the phosphine ligand. The monometallic complex **4** (M = Ni) shows a d–d transition at 440 nm and a charge transfer band at 350 nm (Figure 2).[14] The d–d transitions for the monometallic complexes **4** (M = Pd, Pt) are obscured by the corresponding charge transfer bands at 336 and 280 nm, respectively (Figures 3 and 4).[14]

MLCT (Os → bpy) bands of **1a–d** and **3** are blue-shifted (λ_{max} ~ 470 nm) from that observed for [(bpy)$_3$Os][PF$_6$]$_2$ (λ_{max} = 640 nm) because of the stabilization of the ground state by the enhanced d,π(Os)–d,π(P) back-bonding and the destabilization of the excited state by the poorer σ-donating phosphine ligands.[5a,15] As for the monometallic complex **3**, the charge transfer band (Os → bridging phosphine) of the dimetallic complexes **1a–d** occurs at higher energy than that of the MLCT (Os → bpy). Therefore, photolysis of the dimetallic complexes **1a–d** at low energy (λ > 500 nm) results in selective excitation of the Os^{II} chromophores and production of the ^{3}MLCT excited states.

Excited State Properties. Emission, Quantum Yields, and Excited State Lifetimes. Table 2 summarizes the emission maxima, quantum yields, and excited state lifetimes of these monometallic and dimetallic complexes. The dimetallic complexes **1a–c** exhibit emission characteristics similar to those of the Os^{II} complex **3**; however, the emission of both **1a** and **1b** is strongly quenched (ϕ_{em} = 0.002) and blue-shifted (~20 nm) from that of **2** (ϕ_{em} = 0.049, emission maxima at 625 nm). The dimetallic complex **1c** shows only weak quenching with a ϕ_{em} of 0.044 and an emission maximum at 603 nm, whereas **1d** exhibits a maximum at 603 nm and a ϕ_{em} of 0.063. The blue-shifted emission of the dimetallic complexes **1a–d** correlates well with the "energy gap" as the redox potential difference between the metal-based (Os$^{II/III}$) oxidation and ligand-based (bpy$^{0/-}$) reduction couples increased from 2.61 V in the monometallic complex **3** to ~2.67 V in the dimetallic complexes **1a–d**.[16]

---

[14] Miedaner, A.; Haltiwanger, R. C.; DuBois, D. L. *Inorg. Chem.* **1991**, *30*, 417.

[15] Casper, J. V.; Westmoreland, T. D.; Allen, G. H.; Bradley, P. G.; Meyer, T. J.; Woodruff, W. H. *J. Am. Chem. Soc.* **1984**, *106*, 3492.

Table 2. Excited State Characteristics of Complexes **1a–d** and **3**

	emission max^a (nm)	$\phi_{em}{}^b$	τ (ns)^c
1a	610	0.002	9
1b	605	0.002	12
1c	603	0.044	251
1d	603	0.063	400
3	625	0.049	270

^{a} Emission spectra are obtained by exciting the ^{3}MLCT band (~550 nm) of the samples in the dry, freeze-pump-thawed (five times) or N_2-purged 0.1 M [n-Bu_4N]PF_6/CH_3CN solutions (10^{-4} M) at room temperature. ^{b} ϕ_{em} vs [$Ru(bpy)_3$][PF_6]$_2$ (ϕ_{em} = 0.062). ^{c} Luminescence lifetimes are obtained by exciting the sample in the dry, freeze-pump-thawed (five times) or N_2-purged 0.1 M [n-Bu_4N]PF_6/CH_3CN solutions (10^{-4} M) with a Nd-YAG (532 nm) laser as a pulsed source at room temperature. Excited state lifetimes are determined by a least-squares fit of the exponential decay.

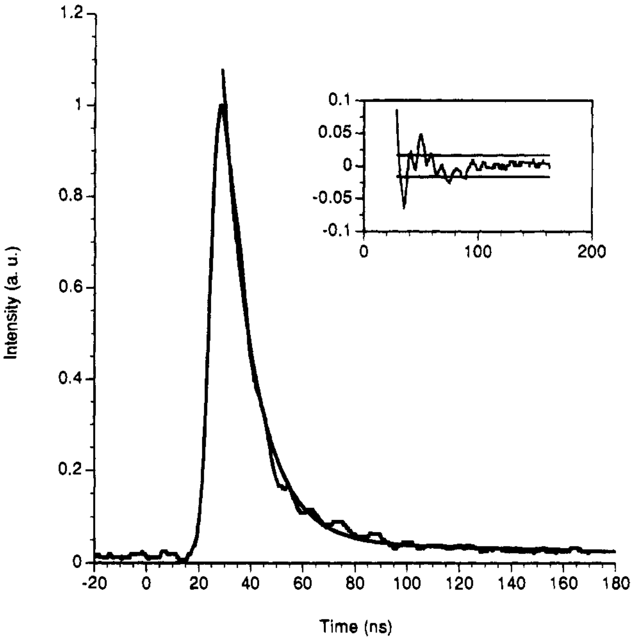

Figure 5. Transient emission spectrum of **1b** (2×10^{-4} M) in a dry, freeze-pump-thawed (five times) solution of 0.1 M [n-Bu_4N]PF_6/CH_3-CN. Conditions: excitation wavelength, 532 nm; power, 10.0 mJ/pulse; slit width, 3 mm.

Transient emission spectra of **1a–d** and **3** are obtained by exciting the ^{3}MLCT band with a Nd-YAG (532 nm) laser pulse. The emission decay traces of **1b**, **1c**, **1d**, and **3** fit to single-exponential curves with lifetimes of 12, 251, 400, and 270 ns, respectively, Table 2. A typical trace and fit (for **1b**) are shown in Figure 5. In contrast, the emission decay trace of **1a** is fit to a biexponential curve to yield lifetimes of 9 and 365 ns, Figure 6. For **1a**, the long lifetime component is assigned to photodecomposition product(s) since emission intensity of that component increased after steady state photolysis (*vide infra*).

Photoinduced Electron Transfer. If there were no interaction between the two bridged metal centers in the excited states of the dimetallic complexes **1a–d**, irradiation of the Os^{II} chromophores should result in photophysical properties that are exactly the same as those of the corresponding monometallic complex **3**. However, this is not the case, as is demonstrated by differences in the emission spectra and excited state lifetimes of these complexes. Because this quenching is independent of concentration under the conditions of the measurement, it is an intramolecular effect, rather than a diffusional quenching.

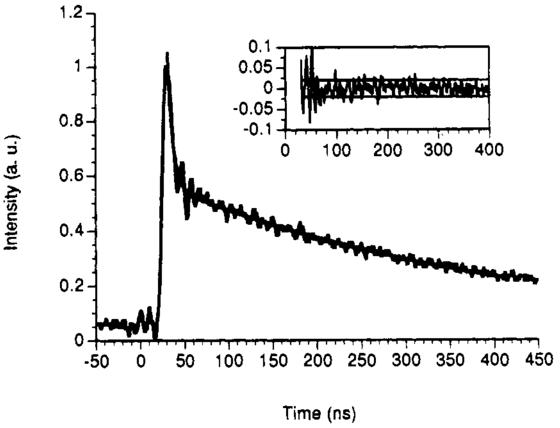

Figure 6. Transient emission spectrum of **1a** (2×10^{-4} M) in a dry, freeze-pump-thawed (five times) solution of 0.1 M [n-Bu_4N]PF_6/CH_3-CN. Conditions: excitation wavelength, 532 nm; power, 10.0 mJ/pulse; slit width, 3 mm.

Scheme 1

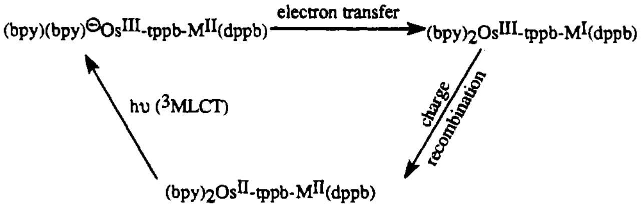

The shortened ^{3}MLCT state lifetimes in **1a–c** are not caused by energy transfer from the $*Os^{II}$ to M^{II} centers (M = Ni, Pd, Pt) because the absorptions of the M^{II} centers do not overlap with the emission of the Os^{II} centers. Instead, quenching is likely to occur by intramolecular electron transfer in the excited state (Scheme 1). Following the initial MLCT excitation of the Os^{II} center, the ^{3}MLCT state can be considered to exist as $(bpy)(bpy^-)Os^{III}-(ppb)-M^{II}(dppb)$. Electron transfer to the M^{II} center (M = Ni, Pd, Pt) produces a transient $(bpy)_2Os^{III}-(tppb)-M^{I}(dppb)$ complex that then relaxes to the ground state, $(bpy)_2Os^{II}-(tppb)-M^{II}(dppb)$, by charge recombination.

The driving force for the intramolecular electron transfer indicated in Scheme 1 cannot be calculated precisely from the values obtained by cyclic voltammetry because the potential of the $M^{II/0}$ couple represents a mean of two component one-electron processes, but the directly relevant $M^{II/I}$ potential must lie negative of the observed waves. At best, a limit for the driving force for electron exchange can be calculated from the available data. From the appropriate reduction potential of the acceptor (the M^{II} center, M = Ni, Pd, or Pt, approximated by the observed potentials for **1a–c**, assigned by analogy with monometallic complex **4**) and excited state oxidation potential of the donor (the $*Os^{II}$ center), an upper limit for ΔG° for intramolecular electron transfer in the excited state of the dimetallic complexes **1a–c** can be calculated, eq 3. The excited

$$-\Delta G^\circ = E_{1/2}(M^{II/I}) - E_{1/2}(*Os^{III/II}) \qquad (3)$$

state oxidation potentials of $*Os^{II/III}$ in the dimetallic complexes **1a–c** are estimated from the emission energies (2.03, 2.05, and 2.06 eV, respectively) and the potentials for the $Os^{II/III}$ couples (1.36, 1.37, and 1.37 V, respectively), Table 3.[4] The reduction potential of the $Ni^{II/I}$ couple is determined as −0.18 V. The reduction potentials of the $M^{II/I}$ couples (M = Pd, Pt) are

---

(16) (a) Dodsworth, E. S.; Lever, A. B. P. *Chem. Phys. Lett.* **1985**, *119*, 61. (b) Dodsworth, E. S.; Lever, A. B. P. *Chem. Phys. Lett.* **1986**, *124*, 152. (c) Kober, E. M.; Caspar, J. V.; Lumpkin, R. S.; Meyer, T. J. *J. Phys. Chem.* **1986**, *90*, 3722. (d) Ciana, L. D.; Dressick, W. J.; Sandrini, D.; Maestri, M.; Ciano, M. *Inorg. Chem.* **1990**, *29*, 2792.

Table 3. Excited State Oxidation Potentials ($E_{1/2}(*Os^{II/III})$), Driving Forces (ΔG°), and Intramolecular Electron Transfer Constants (k_{et}) for the Excited States of the Dimetallic Complexes **1a**–**c**

	$E_{1/2}(*Os^{II/III})$ (eV)[a]	ΔG° (eV)[b,c]	k_{et} (s^{-1})[d]
1a	−0.67	−0.49	1×10^8
1b	−0.68	−0.08	8×10^7
1c	−0.69	+0.07	3×10^5

[a] $E_{1/2}(*Os^{II/III}) = E_{1/2}(Os^{II/III}) - E_{em}$. [b] From eq 3. [c] A calculated upper limit based on the limits for the $M^{II/I}$ potentials imposed by our measured $M^{II/0}$ observed potentials. [d] From eq 4.

determined to be −0.60 and −0.76 V, assuming that the observed reduction potential represents the $M^{II/I}$ couple and that the reduction of the $M^{I/0}$ couple occurs at a less negative potential, Table 1.[6]

Within the uncertainties imposed by this calculation, the intramolecular electron transfers in **1a** and **1b**, Scheme 1, are estimated to be exothermic by approximately 0.49 and 0.08 eV, respectively (Table 3). An electron transfer from the ^{3}MLCT (Os^{II} center) to the Pt^{II} center in **1c** is similarly estimated to be endothermic by approximately 0.07 eV (Table 3). These results are consistent with expectation if the observed luminescence quenching were primarily electron transfer, i.e., with the longer excited state lifetime and higher quantum yield of **1c** than of **1a** or **1b**. The lifetimes of the dimetallic complexes **1a** and **1b** are only 4% that of the monometallic complex **3**, whereas the lifetime of **1c** is nearly the same as that of **3**.

It is therefore likely that the diminished luminescence efficiency in **1a** and **1b** does derive from intramolecular electron transfer. If so, the excited state decay rate can then give a direct measure of the rate of intramolecular electron transfer within the excited states of dimetallic complexes **1a** and **1b**. The electron transfer rate constant (k_{et}) for the dimetallic complexes can be estimated by the difference between the dimetallic complex decay rate, τ_d, and that of the monometallic complex **3**, τ_m (eq 4), Table 3.[1f] The observed electron transfer rate

$$k_{et} = 1/\tau_d - 1/\tau_m \tag{4}$$

constants (k_{et}) are insensitive to the relative driving force (ΔG°) in the dimetallic complexes **1a** and **1b**; the values of k_{et} are of the same order of magnitude (10^8 s^{-1}) for both complexes studied, even though the ΔG° values differ by 0.41 eV, probably because of differences in reorganization energy. Similar results have been observed for an outer-sphere electron transfer between U^{III} and Co^{III}, where the lack of a dependence of the electron transfer rate constants on ΔG° was rationalized by invoking inverted region, tunneling, solvation, and reorganization energy differences.[17]

Photodecomposition of 1a. The increase in the emission intensity of the dimetallic complex **1a** after flash photolysis prompted us to examine the photodecomposition of **1a**. **1a** is completely decomposed after photolysis for 14 h with a 1000 W Xe lamp in a 0.1 M $[n\text{-Bu}]_4PF_6$ solution of CD_3CN/H_2O (5/1).[18] On the basis of the NMR assignments, we believe that the photodecomposition of **1a** was initiated by a dissociation (or decomposition) of the Ni center in the presence of H_2O after electron transfer from the excited Os center in **1a**. The loss of the intramolecular quencher is consistent with the observed increase in emission intensity after prolonged photolysis.

Conclusions

Cyclic voltammetric scans and absorption spectra of dimetallic complexes **1a**–**d** closely resemble those of the (Ni^{II},Ni^{II}), (Ni^{II},Pd^{II}), and (Ni^{II},Pt^{II}) complexes[6] in which intermetallic electronic coupling in the ground state through the 1,2,4,5-tetrakis(diphenylphosphino)benzene ligand is much weaker than in the previously described cyanide- and pyrazine-bridged diruthenium complexes. Nonetheless, substantial intramolecular luminescence quenching of the MLCT state of the Os* center in **1a** and **1b** is observed.

The absence of an energetically appropriate empty orbital (3d of the phosphine ligand and π^* of the benzene ring) in the bridging phosphine ligand disfavors free delocalization into the 1,2,4,5-tetrakis(diphenylphosphino)benzene-bridged dimetallic complexes. Therefore, any intramolecular electron transfer in the excited states of the dimetallic complexes **1a**–**c** mediated by the bridging ligand probably relies less on the presence of a low-lying, empty σ^* orbital in the ligand than on superexchange or tunneling interactions.[19] A reasonable mechanism for the observed quenching of the excited states of dimetallic complexes **1a** and **1b** appears to involve outer-sphere electron transfer between the $*Os^{II}$ chromophore and M^{II} center (M = Ni, Pd). This system is thus similar to a variety of other non-phosphino-bridged dimetallic complexes in which through-bond electronic coupling is more substantial in the excited state than in its ground state precursor.[20]

Acknowledgment. This work was supported by the Office of Basic Energy Sciences, U.S. Department of Energy. We thank Dr. Michael Wolf and Dr. Harold Fox for helpful discussions and for assistance in preparation of the manuscript.

IC9405384

---

(17) (a) Lin, C.-T.; Böttcher, W.; Chou, M.; Creutz, C.; Sutin, N. *J. Am. Chem. Soc.* **1976**, *98*, 6536. (b) Ekstrom, A.; McLaren, A. B.; Smythe, L. E. *Inorg. Chem.* **1975**, *14*, 2899. (c) Marcus, R. A.; Sutin, N. *Inorg. Chem.* **1975**, *14*, 213.

(18) The original peaks at δ 55–60 (m, Ni^{II}-coordinated phosphines) and 29.7 (s) are replaced by the peaks at δ 58 (s), 33.9 (s), 33.2 (s), 30.5 (s), 30.2 (s), 29.7 (s), 29.2 (s), and 24 (s) in the ^{31}P-NMR of the decomposition products. The singlet at 58 ppm is assigned to the monometallic complex **4** (M = Ni),[6] whereas the peaks at 29.7 and 29.2 ppm are assigned to the dimetallic complex **1d**. Similar shifts (δ 30.5, 30.2, 24) are observed in the ^{31}P-NMR spectrum of the small amount (<5%) of isolated decomposition product produced by photolysis of **1a** (with two molecules of hydration) for 6 h in 0.1 M $[n\text{-Bu}]_4PF_6/CD_3CN$.

(19) (a) Casimiro, D. R.; Richards, J. H.; Winkler, J. R.; Gray, H. B. *J. Phys. Chem.* **1993**, *97*, 13073. (b) Winkler, J. R.; Gray, H. B. *Chem. Rev.* **1992**, *92*, 369. (c) Isied, S. S.; Ogawa, M. Y.; Wishart, J. F. *Chem. Rev.* **1992**, *92*, 381. (d) Ogawa, M. Y.; Wishart, J. F.; Young, Z.; Miller, J. R.; Isied, S. S. *J. Phys. Chem.* **1993**, *97*, 11456.

(20) Mecklenburg, S. L.; Peek, B. M.; Schoonover, J. R.; McCafferty, D. G.; Wall, C. G.; Erickson, B. E.; Meyer, T. J. *J. Am. Chem. Soc.* **1993**, *115*, 5479 and references cited therein.